Forest Ecology and Management 571 (2024) 122231

Contents lists available at ScienceDirect

Forest Ecology and Management

journal homepage: www.elsevier.com/locate/foreco

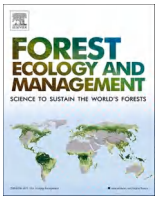

Machine learning-based monitoring of mangrove ecosystem dynamics in the Indus Delta

Ying Zhou [a], Zhijun Dai [a,b,*], Xixing Liang [a,c], Jinping Cheng [d,**]

[a] State Key Laboratory of Estuarine and Coastal Research, East China Normal University, Shanghai 200062, China
[b] Laboratory for Marine Geology, Qingdao Marine Science and Technology Center, Qingdao 266061, China
[c] Guangxi Key Laboratory of Marine Environmental Change and Disaster in Beibu Gulf, Beibu Gulf University (Qinzhou), 200062, China
[d] Department of Science and Environmental Studies, The Education University of Hong Kong, New Territories, Hong Kong, China

ARTICLE INFO

Keywords:
Mangrove expansion
Hydro-sediment dynamic
Machine Learning
Random Forest
Tidal channel
Shoreline erosion

ABSTRACT

Mangrove forests play a vital role in carbon sequestration, typhoon-induced wave attenuation, and the provision of ecological services. However, mangrove ecosystems have experienced large-scale loss globally due to rising sea levels and anthropogenic activities. This study investigates the dynamic changes in mangrove cover within the mega-Indus delta, the largest delta in Pakistan and Southern Asia, using multi-temporal remote sensing data and machine learning techniques from 1988 to 2023. The results indicate an increasing trend in mangrove areas in the Indus Delta, with an average annual growth rate of 18.72 %. The spatial distribution of mangrove forests tends to concentrate towards the landward areas, extending along tidal channels, while losses primarily occur in the seaward regions. Rising sea levels pose a potential threat to the survival of these mangroves. The strong southwest monsoon-driven waves are the leading cause of shoreline erosion of the Indus Delta mangroves. Meanwhile, the reduction in riverine sediment discharge is not associated with the increase in mangrove area. Instead, the tidal currents influenced by the southwest monsoon carry sediments into the delta's tidal channels, causing them to fill and create suitable habitats for mangroves, which are the primary drivers of the observed mangrove expansion in the Indus Delta. Additionally, afforestation activities observed in the northwest and southwest parts of the study area have contributed to the restoration of mangroves. The loss of mangroves in the northernmost part of the northwest region was attributed to an oil spill incident. This study highlights the dynamic nature of mangrove ecosystems in the Indus Delta, characterized by an arid climate and low population density. The findings provide valuable insights into the factors influencing mangrove gain and loss and can inform management strategies for global mangrove restoration efforts.

1. Introduction

Mangrove ecosystems in intertidal zones of tropical and subtropical coastlines represent a unique transition zone between terrestrial and marine environments (Giri et al., 2011). These ecosystems provide essential habitats for various terrestrial and marine organisms (FAO, 2007). Mangrove forests play a crucial role in coastal protection, effectively trapping sediment accumulation and mitigating storm surge impacts on intertidal flats (Chaudhuri et al., 2019). They also contribute to shoreline stability (Raju and Arockiasamy, 2022). Furthermore, mangrove ecosystems possess a remarkable capacity for carbon sequestration, exceeding that of many other ecosystems (Ezcurra et al., 2016; Song et al., 2023). This significant carbon storage potential makes them crucial for mitigating climate change. However, global mangrove forests are facing significant threats due to rising sea levels and increasing anthropogenic pressures (Ward et al.,2016; Blankespoor et al., 2017; Goldberg et al., 2020). Over the past 30 years, the world's mangrove forests have decreased by 10,400 square kilometers, with an annual loss rate of 212 km^2 over the past decade (FAO, 2020). There is an urgent need to monitor dynamic changes in mangrove forests worldwide. Such monitoring efforts can inform restoration initiatives for damaged mangrove ecosystems and contribute to the development of effective policies for enhanced mangrove forest protection.

Recent research has focused on the dynamic changes occurring

* Corresponding author at: State Key Laboratory of Estuarine and Coastal Research, East China Normal University, Shanghai 200062, China.
** Corresponding author.
E-mail addresses: zjdai@sklec.ecnu.edu.cn (Z. Dai), jincheng@eduhk.hk (J. Cheng).

https://doi.org/10.1016/j.foreco.2024.122231
Received 26 June 2024; Received in revised form 19 August 2024; Accepted 20 August 2024
Available online 24 August 2024

within mangrove ecosystems (Bryan-Brown et al., 2020; Bunting et al., 2023; Contessa et al., 2023). Globally, Indonesia, Malaysia, Myanmar, Thailand, the United States, Mexico, India, Cuba, and the Philippines have experienced the highest rates of mangrove loss (Bryan-Brown et al., 2020). Mangrove loss has also been documented in South America, Oceania, and Africa (Bunting et al., 2023; Contessa et al., 2023). Conversely, some regions have shown an increase in mangrove cover (Shapiro et al., 2015; Wang et al., 2021). Studies have observed both landward retreat and seaward expansion of mangroves in various delta systems. The Ganges and Mekong Deltas have shown a landward retreat of mangroves (Besset et al., 2019; Samanta et al., 2021), although other deltas have experienced seaward expansion (Long et al., 2021; Xiong et al., 2024). This variability suggests that mangrove dynamics are complex and influenced by multifaceted factors (Hagger et al., 2022).

Previous research has identified several factors contributing to mangrove loss. High salinity soils resulting from reduced rainfall could induce a low survival rate of mangroves (Field, 1995). Rising sea levels have driven mangroves to retreat landward (Gilman et al., 2007), while extreme storm events have led to widespread mangrove die-offs (Paling et al., 2008). Insufficient sediment supply has been implicated in the retreat of mangrove shorelines (Besset et al.,2019). However, some studies have documented mangrove growths in inland areas far from the coastline, particularly around tidal channels (Visschers et al.,2022). Furthermore, Lee et al. (2022) observed that mangrove expansion can lead to a transition in tidal channels from a wider, meandering state to a narrower, straighter configuration.

In addition to natural factors, human activities have significantly impacted mangrove ecosystems. Reclamation, aquaculture, and industrial pollution have contributed to the decline of mangrove forests (Maiti and Chowdhury, 2013; Richards and Friess, 2016; Slamet et al., 2020). However, mangrove restoration and replanting projects, driven by conservation policy implementation in some countries, have resulted in the recovery and expansion of mangrove forests in various regions (Ellison et al., 2020; Gerona-Daga and Salmo, 2022).

The dense, prop root structure of mangroves, coupled with their periodically submerged muddy terrain, poses challenges for traditional field survey methods, limiting the scope and comprehensiveness of monitoring efforts (You et al., 2023). In recent years, advancements in terrestrial satellite data have significantly improved the temporal accuracy and spatial resolution for quantifying changes in the Earth's surface, including natural and anthropogenic alterations (Wulder et al., 2019). This data has proven valuable in the study of coastlines and various habitats (Tang et al., 2016; Zhang and Hou, 2020; Zheng et al., 2023). Remote sensing has emerged as a powerful tool for mangrove observation (Pham et al., 2019; Wang et al., 2019; Yang et al., 2022a). However, challenges remain in identifying submerged mangroves during tidal cycles and limitations in remote sensing image resolution. To address these challenges, random forest and threshold segmentation have been incorporated into such studies (Liu et al., 2021; Jia et al., 2023; Zablan et al., 2023; Xiong et al., 2024). The continuous improvement in mangrove datasets also holds significant promise for global conservation and restoration of mangroves (Worthington et al., 2020). Despite extensive studies on mangrove forest changes in various coastal regions, limited information exists on the dynamics of mangroves in the Indus Delta, the largest delta of Pakistan, located in Southern Asia. The Indus Delta supports a population of approximately 300,000 residents (Karrar, 2021). The Indus Delta's mangrove ecosystems are crucial for maintaining Pakistan's ecological and social well-being.

This study focuses on the Indus Delta as the study area, utilizing satellite remote sensing data from 1988 to 2023 to extract mangrove information using deep learning methods. The objectives of this study are to 1) quantify the temporal and spatial changes in the mangrove area within the Indus Delta; 2) determine the erosion and accretion status of the mangrove ecosystem; 3) explore the underlying drivers of mangrove gain and loss. The study will shed light on the damage and activity dynamics of mangroves in the Southern Asian Indus Delta, which will provide valuable insights for mangrove government departments worldwide, facilitating mangrove restoration efforts and policy development.

2. Materials and methods

2.1. Study area

The Indus River, originating from the Tibetan Plateau and traveling the Himalayas and the Karakoram Range, flows through Pakistan, Afghanistan, India, and China, before reaching the Arabian Sea. Pakistan encompasses occupies 56 % of the Indus River Basin. The Indus Delta, located in the Sindh province of Pakistan (Fig. 1A), exhibits a fan-shaped morphology attributed to the extensive sediment deposition from the upstream mountainous regions (Kalhoro et al., 2016). The Indus Delta comprises 17 main creeks and tributaries (Amjad and Jusoff, 2007). However, after the construction of a series of upstream hydraulic engineering projects, only two active creeks remain, namely Khobar and Khar (Siyal et al., 2022), with Khobar serving as the main channel for Indus River outflow. The southwest monsoon contributes significant precipitation to the delta (Inam et al., 2007).

The study area, situated in a subtropical region with an arid climate and limited rainfall, covers an area of 6411.267 km^2, extending from Korangi Creek to Sir Creek. The two main creeks, Khobar Creek and Wari Creek, divide the study area into three sections: the Northwest Part (NWP), the Southwest Part (SWP), and the South Part (SP) (Fig. 1B). The annual average rainfall is 160 mm. The nearest tide gauge station in Karachi recorded a tidal range of 2.7 m, characterized by a mixed semidiurnal tide with two high tides and two low tides daily (Syed and Siddiqa, 2019). Extensive branching tidal creeks dominate the northern delta, influenced by tides, while broader channels penetrating further inland are observed in the southeastern part. Tidal channels are densely distributed from the northwest to the southeast, constituting a system significantly influenced by waves and tides (Giosan et al., 2006).

As a representative arid climate delta, the Indus Delta's formation and evolution have been shaped by historical climate change, human activities, and hydrological and geomorphological alterations. The delta was initially formed during humid periods due to sediment accumulation. However, the river's input into the delta has decreased due to arid climate conditions and large-scale irrigation projects. Since the late 19th century, extensive engineering constructions have significantly reduced the flow and sediment supply to the delta, leading to a developed tidal river network and coastal erosion (Day et al., 2021). The shortage of freshwater and insufficient sediment supply have negatively impacted the delta's ecological and economic sustainability, particularly affecting the mangrove ecosystems and the fisheries (Hadi, 2019). Given the multifaceted stressors facing the Indus Delta, studying its ecological evolution, particularly changes in mangroves, is of paramount importance and urgency.

2.2. Materials

Google Earth Engine (GEE) provides a highly practical and efficient platform for analyzing remote sensing data within the context of geographic big data (Yang et al., 2022b). Specifically, GEE's robust computational and storage capabilities facilitate the processing of large-scale spatial data. Additionally, its support for batch processing using JavaScript or Python streamlines the workflow, eliminating the need for cumbersome traditional data preprocessing and significantly enhancing work efficiency (Teluguntla et al., 2018). This leveraged GEE's extensive remote sensing data archive, including Landsat 5 TM, Landsat 8 OLI, and Landsat 9 OLI-2, to acquire multiple cloud-free images from 1988 to 2023. The study area consistently covered the same geographic area (path 152, row 43). Image preprocessing employed the 1984 World Geodetic System (WGS 84) as the geographic coordinate

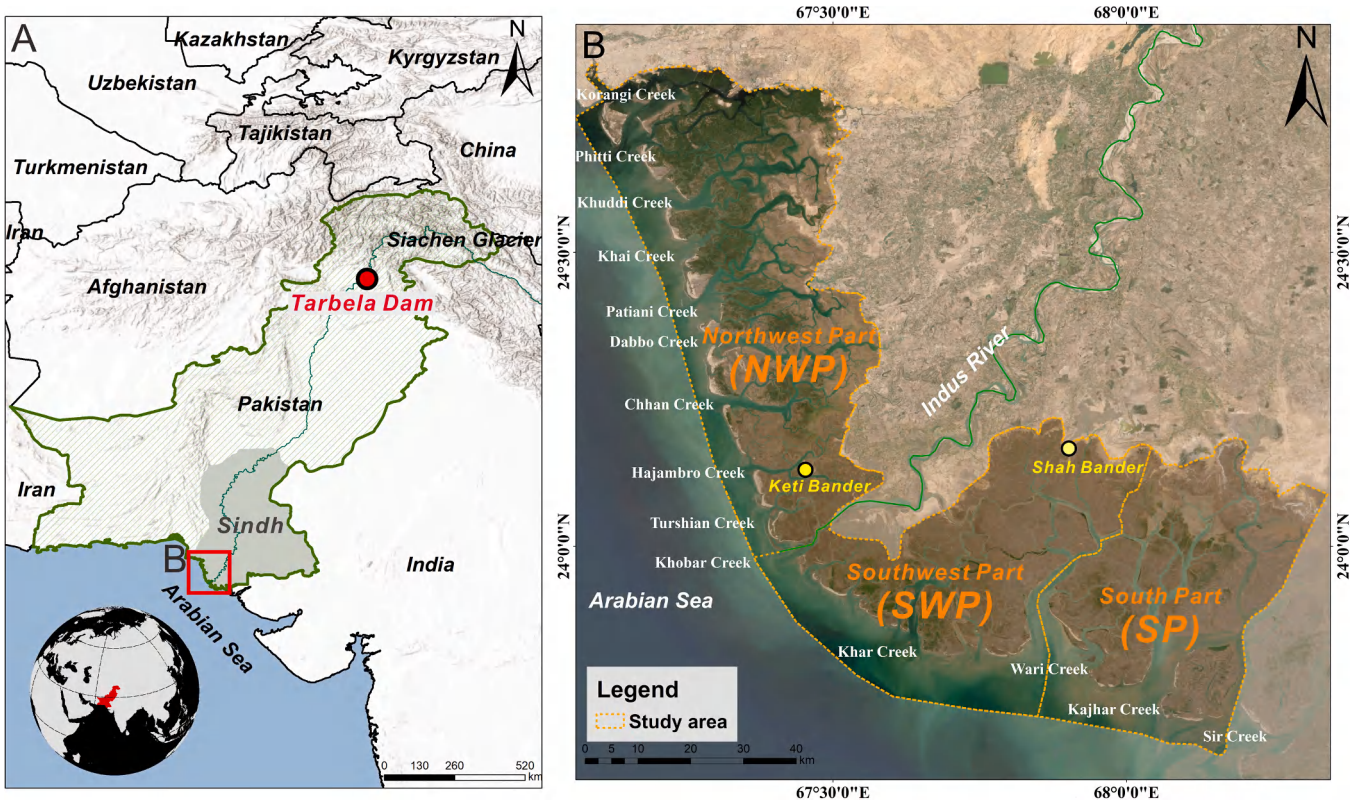

Fig. 1. Map of the Indus Delta (A) and study area (B).

system and the WGS_1984_UTM_Zone_42N of the Universal Transverse Mercator (UTM) as the projected coordinate system. However, no remote sensing images were available during 2003–2007 and 2012.

To validate the accuracy of mangrove identification, this study utilized the global mangrove watch dataset (https://www.globalmangrovewatch.org/) and historical imagery from Google Earth to establish sample points. Sediment discharge data for the Indus River entering the sea were obtained from remote sensing-derived estimates of suspended sediment flux into the sea (Dethier et al., 2022). Meanwhile, wave direction and significant height of waves (SHW) were obtained

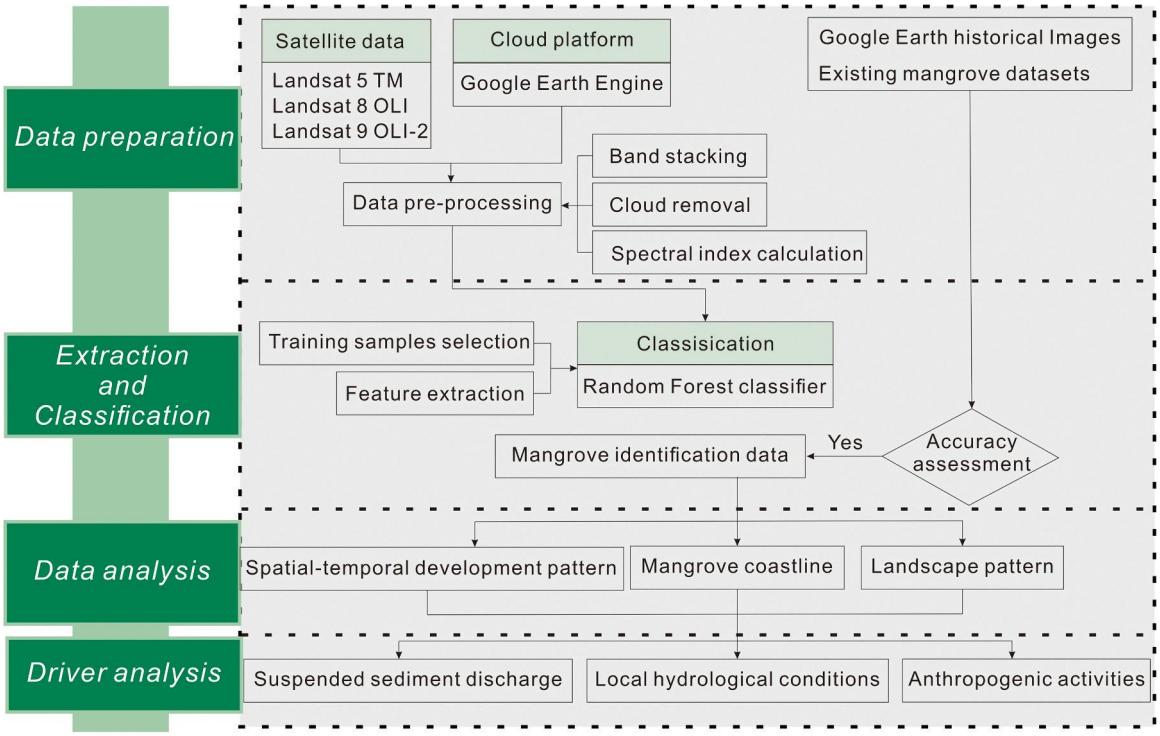

Fig. 2. Schematic methodological framework employed in the study.

from the European Centre for Medium-Range Weather Forecasts (ECMWF) (https://cds.climate.copernicus.eu/cdsapp#!/home). Sea current field data were downloaded from Copernicus Marine Environment Monitoring Service (CMEMS)(https://data.marine.copernicus.eu/product/GLOBAL_MULTIYEAR_PHY_001_030/description).

2.3. Methods

2.3.1. Methodological framework

This study's methodology utilizes a framework that integrates remote sensing images on the Google Earth Engine platform with deep learning algorithms to identify mangroves in the Indus Delta. The methodology comprises four main steps (1) Data preparation; (2) Extraction and Classification; (3) Data analysis; (4) Driver analysis. The overall methodology is illustrated in Fig. 2.

2.3.2. Random forest

Machine learning has become increasingly prevalent in Earth sciences, with popular classification algorithms including Support Vector Machines (SVMs), ensemble classifiers (e.g., ensemble learning methods), and deep learning algorithms (Sheykhmousa et al., 2020). Each algorithm possesses unique strengths and limitations. SVMs excel in handling high-dimensional data with relatively small sample sizes but require significant computational resources. Ensemble learning methods enhance accuracy and robustness by combining multiple models, reducing overfitting but demanding substantial computational resources and fine-tuning. Deep learning algorithms excel in processing complex, nonlinear relationships in image data but require extensive data and computational resources and offer limited interpretability.

The Random Forest method has gained prominence in Earth science research due to its high accuracy, robustness, and computational efficiency. Several studies have demonstrated its effectiveness in mangrove identification compared to other classification algorithms (Poortinga et al., 2020; Habibullah et al., 2023). Random Forest, an ensemble learning method, constructs multiple decision trees and aggregates their results through voting, leading to excellent overall performance (Fernández-Delgado et al., 2014). It is less prone to overfitting with high-dimensional data and effectively handles imbalanced samples. Additionally, Random Forest provides feature importance evaluation, aiding researchers in understanding the model's decision-making process and classification results (Belgiu and Drăguţ, 2016).

This study utilizes the Random Forest method for classifying and recognizing remote sensing images, focusing on the spatiotemporal changes of mangroves in the Indus Delta. Google Earth Engine (GEE), a powerful geospatial analysis platform, provides extensive support for various supervised classification algorithms, including Random Forest. To study mangrove spatiotemporal changes, preprocessed satellite images were used, and training points were manually created in GEE, labeling different land cover types. The "Random Points" command generated random points, with approximately 70% used for training the Random Forest classifier and the remaining 30% for evaluating its accuracy in identifying mangroves. This approach enables efficient processing of large-scale remote sensing data and provides insights into the importance of various variables during classification, offering valuable scientific data support for mangrove conservation and management.

2.3.3. Mangrove shoreline analysis

To analyze the spatial distribution of mangrove gains and losses, this study employed ArcGIS software's Analysis Tools, specifically the Erase option within the Overlay tool. By erasing the previous year's layer with the subsequent year's layer, the output reveals new layers that indicate the increase in mangroves during that period. Conversely, the result shows the loss of mangroves.

Mangrove shoreline is a key indicator for assessing coastal changes. This study employed the Digital Shoreline Analysis System (DSAS) to evaluate the edge changes of mangroves over several years. DSAS tools are widely recognized for their effectiveness in assessing coastline changes (Rahman et al., 2022). Mangrove shorelines were extracted for the years 1988, 1993, 1998, 2002, 2008, 2013, 2018, and 2023. The Digital Shoreline Analysis System, developed by the United States Geological Survey (USGS), operates within the ArcGIS software. DSAS supports the analysis and processing of various statistical indicators, including Linear Regression Rate (LRR) and Endpoint Rate (EPR) (Thieler et al., 2009).

2.3.4. Landscape pattern

Quantitative landscape pattern analysis plays a crucial role in understanding the ecological processes within a landscape (Šímová and Gdulová, 2012). This study employed Patch Density (PD) and Cohesion Index (COHESION) to measure the landscape pattern characteristics of mangroves in the study area. Fragstats software, a powerful tool for landscape pattern analysis, was used to calculate these indicators. Patch Density (PD) serves as an indicator of landscape fragmentation and heterogeneity. Within a given landscape area, a higher patch density indicates landscape dispersion, while a lower patch density indicates landscape aggregation. The Cohesion Index (COHESION) measures the aggregation of landscape distribution, revealing whether patches are connected. The formulas for both indicators are as follows (McGarigal et al., 2002):

$$PD = \frac{N}{A}(10000)(100) \tag{1}$$

$$COHESION = \left[1 - \frac{\sum_{i=1}^{n} P_i}{\sum_{i=1}^{n} P_i\sqrt{a_i}}\right] \bullet \left[1 - \frac{1}{\sqrt{N}}\right]^{-1}(100) \tag{2}$$

Where, N: total number of patches of the selected patch type landscape, A: total area of the landscape, i: 1, …, n patches, ai: the area of patch i, Pi: the perimeter of patch i.

2.4. Computational Environment and Resource Allocation

Google Earth Engine (GEE) (https://earthengine.google.com) is a cloud-based platform for Earth science data and analysis. GEE has a built-in random forest classification algorithm, which can be accessed using the ee.Classifier.smileRandomForest function to extract mangroves in the study area. This allows users to perform data processing and classification directly on the platform, ensuring data consistency and integrity. The scripts for GEE are primarily written in JavaScript. We wrote and executed scripts in the GEE Code Editor to process remote sensing images, train classification models, and conduct time series analyses. In this study, the latest version of Google Chrome browser was used to ensure compatibility with the GEE platform and optimal performance. All data processing and analysis were carried out within the Google Earth Engine's cloud computing environment. Although the GEE platform is cloud-based, with computation tasks executed by Google's servers, the local computing environment still has a certain impact on the smooth progress of the research. We maintain at least 50 GB of available storage space locally to save scripts and processed data files temporarily. Through this cloud computing architecture, we were able to efficiently handle large-scale data and obtain analysis results in a relatively short time.

3. Results

3.1. Variations in mangrove forest area

The mangrove forest area showed an increasing trend, expanding from 433.22 km^2 in 1988–838.63 km^2 in 2023, indicating a net growth of 405.41 km^2 (Fig. 3). Initially, the mangrove forest coverage was

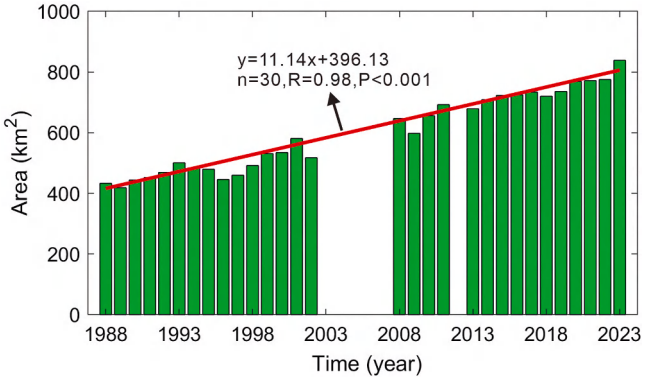

Fig. 3. Variation of mangrove forest area within the Indus Delta from 1988 to 2023.

433.22 km^2 in 1988, which increased to 500.97 km^2 in 1993, reflecting an annual growth rate of 2.95 %. However, a slight decrease was observed from 500.97 km^2 in 1993–491.96 km^2 in 1998. From 1998–2002, the mangrove forest area experienced an increment of 25.60 km^2, with an annual growth rate of 1.28 %. Subsequent years demonstrated relatively stable growth rates: 3.79 % from 2002 to 2008, 0.97 % from 2008 to 2013, 1.18 % from 2013 to 2018, and 3.09 % from 2018 to 2023, respectively (Fig. 3).

Moreover, the spatial analysis revealed distinct variations in the mangrove area within the Indus Delta (Fig. 4). In the northwest part (Fig. 4A), the area of mangroves increased from 330.23 km^2 in 1988–574.84 km^2 in 2023. This growth was characterized by a rapid expansion from 1988 to 2002, followed by a gradual stabilization from 2008 to 2023, transitioning into a steady growth phase. Conversely, in the southwest region (Fig. 4B), the area of mangroves expanded also showed from 21.78 km^2 in 1988–160.19 km^2 in 2023. Unlike the northwest part, the southwest region experienced an initial phase of steady growth, followed by a rapid expansion phase. In contrast, the south part (Fig. 4C) demonstrated a continuous in mangrove area throughout the study period.

3.2. Gain and loss in mangrove forest area

From 1988–2023, the mangrove forest area in the study region exhibited an overall increasing trend, with a net expansion of 499.60 km^2 and a reduction of 94.19 km^2 (Fig. 5). During the period from 1988 to 1993, the spatial distribution of the mangrove forest area exhibited net gains, with. an increase of 123.53 km^2 and a loss of 55.78 km^2. The gains were predominantly concentrated in the northwest and the southern parts, while minor losses were observed in certain coastal areas. From 1993–1998, losses were mainly concentrated in the southwest part of the mangrove forests established in 1993. Despite these losses, the regions experiencing growth remained consistent with the 1988–1993 period, indicating that the spatial dynamics of the mangrove forests were still relatively unstable, though growth areas became more focused. From 1998–2002, a noticeable trend of mangrove loss towards the sea was observed, with an area increase of 101.12 km^2 and a loss of 75.52 km^2. These seaward losses were particularly evident in the southwest and southern parts.

Subsequently, the spatial expansion of mangrove areas continued to progress, albeit at varying rates. From 2002–2008, the mangrove area increased by 191.57 km^2 and decreased by 62.20 km^2, with overall growth dominating. Notably, the growth extended inland along tidal channels, particularly in the southwest part. From 2008–2018, the rate of mangrove area expansion slowed: from 2008 to 2013, the area increased by 81.45 km^2 with a loss of 49.29 km^2, and from 2013 to 2018, the area increased by 95.98 km^2 with a loss of 54.82 km^2. During this period, the original mangroves remained stable, and their distribution continued to expand along tidal channels. From 2018–2023, the mangrove area increased by 166.69 km^2 and lost 48.30 km^2, resulting in the current distribution pattern. Overall, from 1988 to 2023, the distribution of mangroves became more concentrated, with changes in spatial distribution primarily occurring in the southwest and southern parts of the study area. The increases in mangrove area mainly occurred inland, extending upwards along tidal channels, while losses predominantly occurred towards the sea.

3.3. Shoreline change in mangrove forest

Shoreline changes in the mangrove forests were analyzed for the years 1988, 1993, 1998, 2002, 2008, 2013, 2018, and 2023, resulting in the generation of 1095 transects (Fig. 6). Positive change rates of the shoreline indicate accretion of the mangrove forest edge, while negative change rates indicate erosion. The average total migration rate from 1988 to 2023 was −4.7 m/yr. Analysis revealed 592 transects showing erosion and 503 indicating accretion. The proportion of erosion to accretion sections was 54.06–45.94 %, with average change rates of −28.12 m/yr and 22.85 m/yr, respectively. Moreover, the erosion and accretion of the mangrove forest shoreline alternated, with the most pronounced erosion observed in the southwest and south coastal areas. Overall, despite some seaward expansion of the mangrove forest shoreline, the general trend indicates erosion, demonstrating a net retreat towards the land.

It is worth noting that the change rates varied across different regions. The northwest part of the study area, situated on the right bank of the Indus River, experienced the least erosion. In contrast, the southwest and south parts, located on the left bank, exhibited higher erosion rates. The southwest area, in particular, faced the most severe erosion, with a rate of 35.42 m/ yr, followed by the south region, while the northwest part experienced the least erosion (Fig. 7).

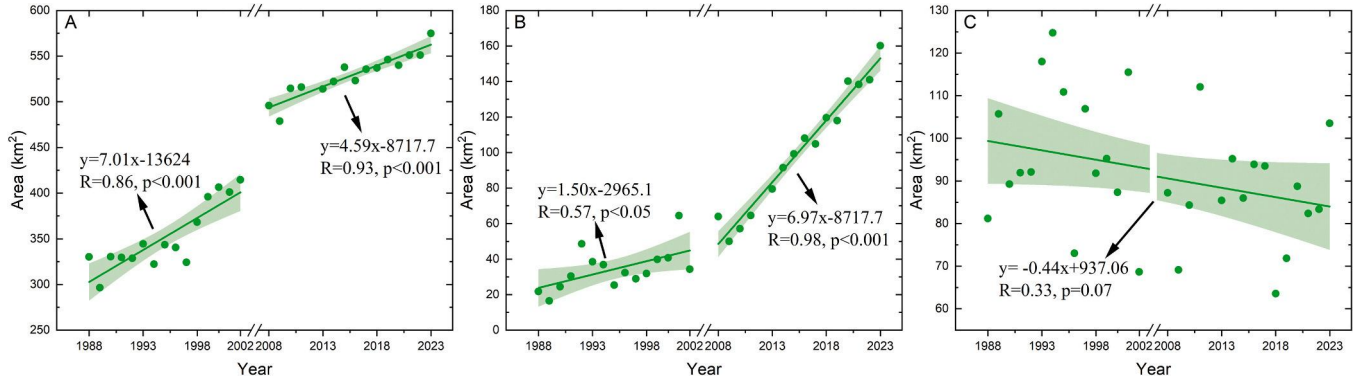

Fig. 4. Temporal changes in mangrove area across different regions of the Indus Delta, including Northwest Part (A), Southwest Part (B), and South Part (C).

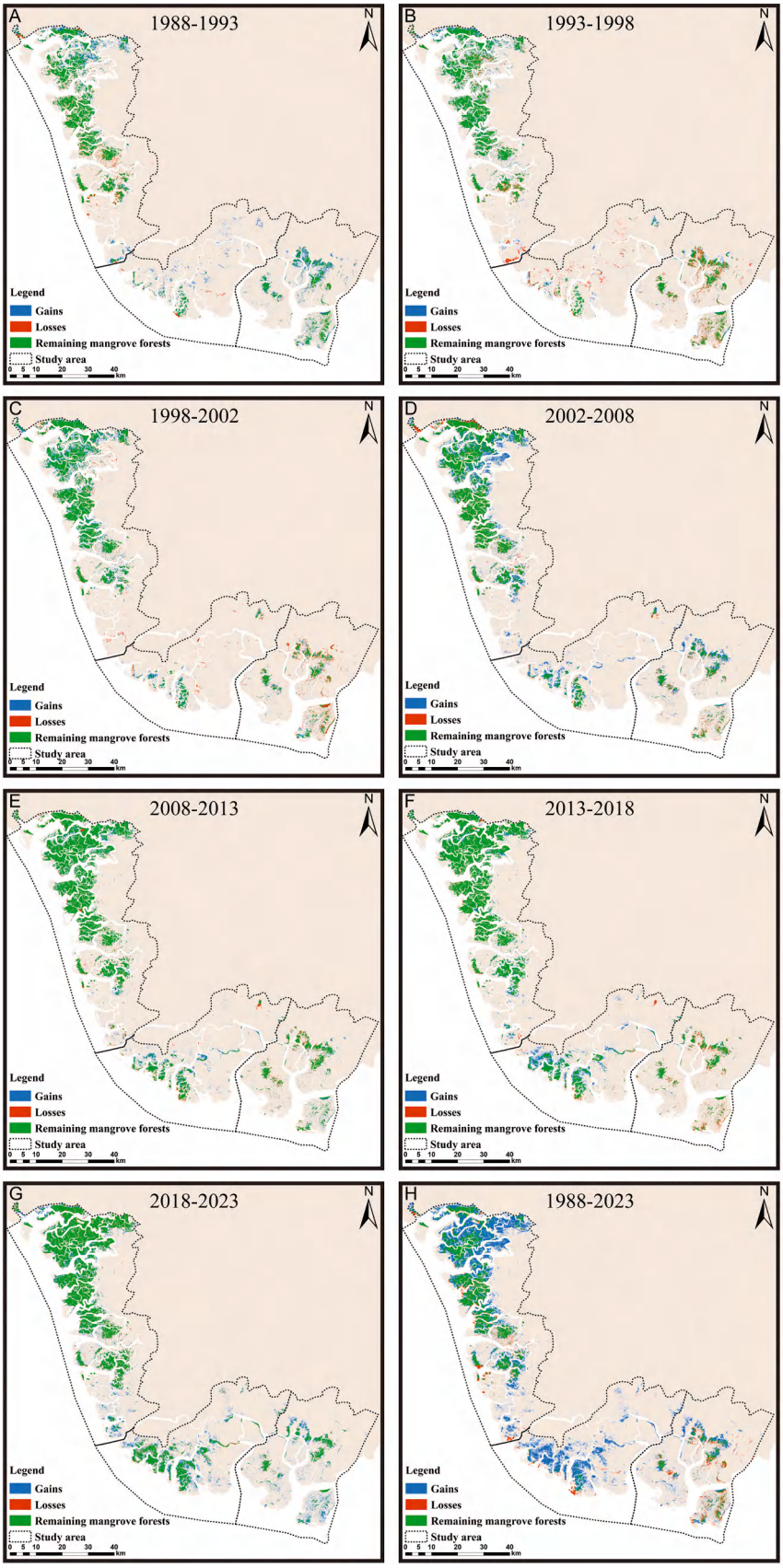

Fig. 5. Spatial distribution of gains and losses of mangrove forest area within the Indus Delta from 1998 to 2023. A-H: Spatial distribution of mangrove forests at different periods during 1988–2023.

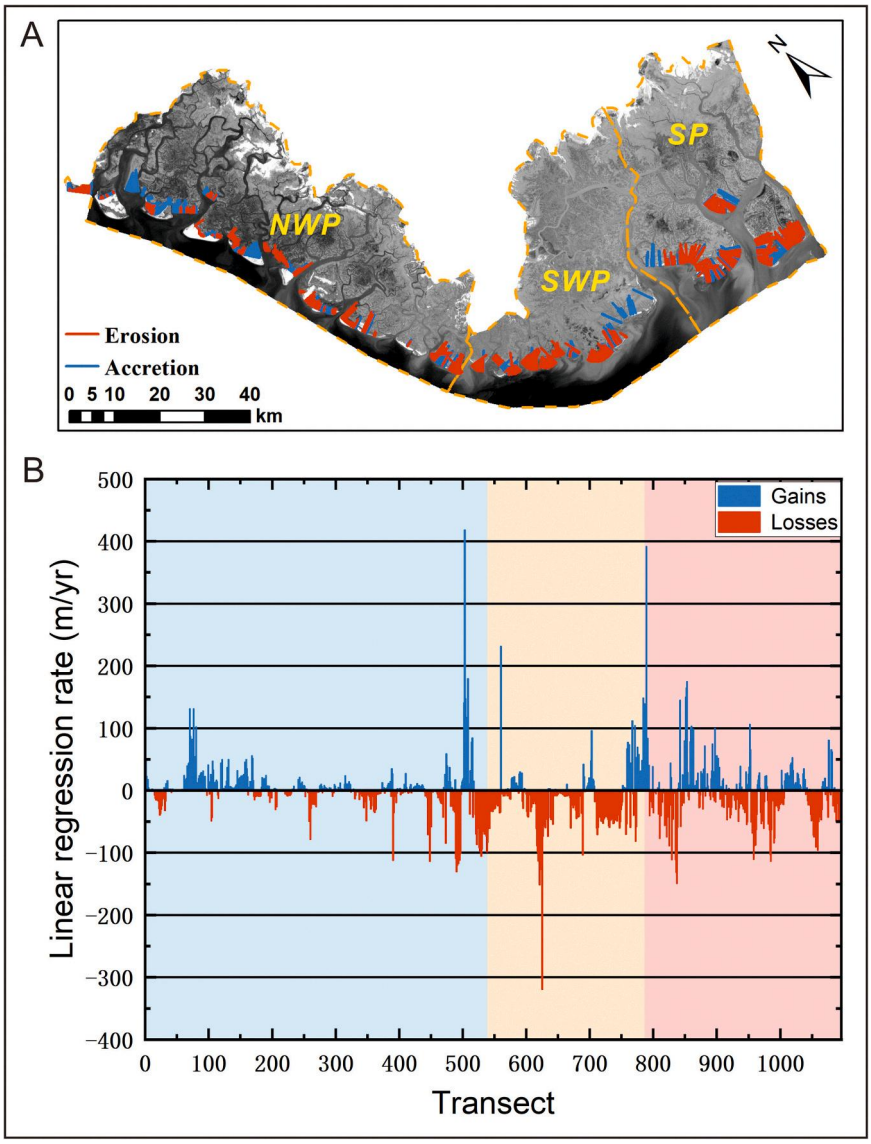

Fig. 6. (A) The erosion and accretion of the mangrove shoreline of the Indus Delta from 1988 to 2023, categorized by region: Northwest Part (NWP), Southwest Part (SWP), and South Part (SP). (B) Quantitative analysis of shoreline gains and losses of the Indus Delta from 1988 to 2023.

3.4. Landscape pattern change in mangrove forest

Landscape pattern indices were employed to reveal the vegetation distribution characteristics of the region, with each indicator providing unique insights. Patch density (PD), which is directly proportional to the degree of spatial fragmentation of the landscape, serves as a proxy for human-induced disturbances to the landscape (Nrothwest, 1995). From 1988–2023, the patch density of the Indus Delta exhibited a decreasing trend, declining from 1.31 in 1988–0.88 in 2023 (Fig. 8A). This decrease indicates a trend toward the concentration of mangroves over the study period, consistent with the spatial distribution of mangroves from 1988 to 2023. The aggregation index (COHESION) showed a linear increase from 99.63 in 1988–99.73 in 2023 (Fig. 8B), signifying an enhancement in the overall interconnectedness of mangroves.

4. Discussion

4.1. Impacts of suspended sediment discharge from upstream

The long-term viability of mangrove ecosystems is intrinsically linked to the availability of sediment (Spalding et al., 2014). However, anthropogenic hydraulic interventions have significantly disrupted mangrove connectivity and impeded the supply of essential sediment and nutrients (Anthony and Goichot, 2020). Following Pakistan and India signing the Indus Waters Treaty in 1960, extensive west-to-east hydraulic projects, including the construction of reservoirs and dams on the upper Indus River, were initiated. Since the operation of the Tarbela Dam in 1976, the average river flow of the Indus River has decreased to merely 2.9 % of its pre-dam levels (Ahmad and Center, 2012). This substantial reduction in river flow has critically impaired sediment transport to estuarine areas, contributing to the observed decline in mangrove coverage from 1988 to 2023. This trend is illustrated by the retreat of the mangrove shoreline on the seaward side (Fig. 6), underscoring the reduction in upstream sediment transport as a primary causative factor.

Inadequate sediment supply exacerbates the erosion of muddy substrates, causing shoreline retreat. When sediment deficits surpass critical thresholds, the dynamic equilibrium of mangrove coastlines is disrupted, posing a significant threat to the sustainability of these mangrove ecosystems (Ellison, 2021). Between 1988 and 2023, a decreasing trend in suspended sediment discharge from the upper reaches of the Indus River was observed (Fig. 9 A), whereas the overall area

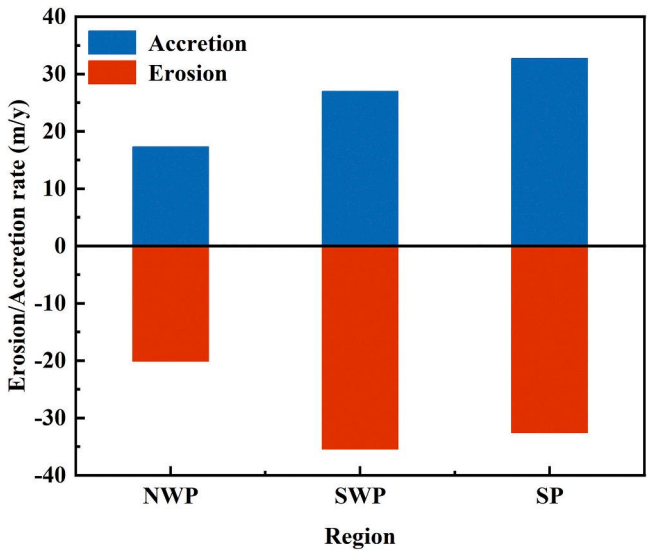

Fig. 7. Quantitative analysis of shoreline gains and losses in different regions of the Indus Delta from 1988 to 2023. Northwest Part (NWP), Southwest Part (SWP), and South Part (SP).

of mangroves has increased. A negative correlation between the area of Indus River mangroves and the suspended sediment discharge (Fig. 9B) indicates that the reduction in upstream sediment delivery has not directly led to a decrease in the downstream delta mangrove area. Therefore, other factors affecting mangrove area changes in the Indus River delta warrant consideration.

4.2. Impacts of the local hydrological conditions

Analysis of wave direction diagrams for the northwest, southwest, and southern parts of the study area (Fig. 10) reveals a predominance of southwestward waves. In the southwest, 58.73 % of the southwestward waves exceed a significant wave height of 1 m, with some waves over 4 m (Fig. 10), likely driving the extensive seaward mangrove loss observed. The erosion rates in the southwest and south regions, at −35.42 m/yr and −32.60 m/yr, respectively (Fig. 7), are particularly pronounced due to persistent southwest wave action. This wave-induced scarp formation is evident along the mangrove shorelines in these regions (Fig. 11).

Despite the reduction in sediment transport to the delta estuary, mangrove areas have continued to expand, likely due to tidal actions resuspending sediments (Reynaud and Dalrymple, 2012). Tidal currents, flowing southeast as observed in multi-year average sea surface current maps from 1993 to 2023 (Fig. 12), facilitate sediment deposition and compensate for upstream sediment deficiencies. The left bank of the Indus, the delta's southwest and south parts (Fig. 1B), is most affected by tidal currents throughout the year. During summer, the southwest monsoon further enhances inland tidal flow, bringing sediments into tidal channels at flow rates up to 0.25 m/s. This sediment transportation process by tidal current can induce the filling of tidal channels and create a suitable habitat for mangroves along tidal channels (Woodroffe, 1992). Tidal currents and wave action jointly influence sediment distribution and transport pathways in the study area. Strong wave action suspends sediment, increasing the concentration of suspended sediment, which tidal currents then transport inland. The interaction fosters mangrove growth, as evidenced by the expansion of mangroves occupying the tidal channel waters, causing the tidal channel shrinkage (Fig. 13).

Mangrove growth along tidal creeks in the northwest, southwest, and southern parts of the study area, has been observed from 1988 to 2023 (Fig. 13). Extensive tidal flats and dynamic tidal changes have promoted the formation and evolution of tidal channels. From 1988–1998, mangroves in the three regions began to show sporadic or small-scale landward expansion, with the northwest being the most notable area for this expansion. During high tides, water pushes upstream, leading to sediment deposition on tidal flats due to the slower flow velocity. This deposition during high tides, combined with erosion during low tides, has deepened channels and promoted tidal channel extension in the northwest (Fig. 13A1). From 1998–2008, the tidal channels in the northwest began to connect (Fig. 13A2), while those in the southwest and south narrowed (Fig. 13B2, 13C2), promoting the landward expansion of the mangroves. The northwest mangroves began to show block-like aggregation, and the southwest clearly showed strip-like extension along the tidal channels (Figs. 5C, 5D). From 2008–2023, the tidal creek waters in the northwest continued to expand, further connecting tidal channels and stabilizing mangrove growth (Fig. 13A3-A5). Concurrently, mangroves in the southwest and southern regions continued to grow along these tidal channels (Fig. 13B3-B5; Fig. 13 C3-C5). The mangrove expansion in the three regions tended to stabilize, with most areas transitioning into long-term stable mangroves (Fig. 5E-G). Overall, as the tidal channels in the northwest gradually connect (Fig. 13D), the upstream flow of the tide brings saline water that impacts the mudflats, transforming them into tidal flats. Avicennia marina, constituting 95 % of the mangrove species in the Indus Delta (Mukhtar and Hannan, 2012), uses its unique salt glands to expel salt through osmosis, maintaining the osmotic pressure balance and enabling

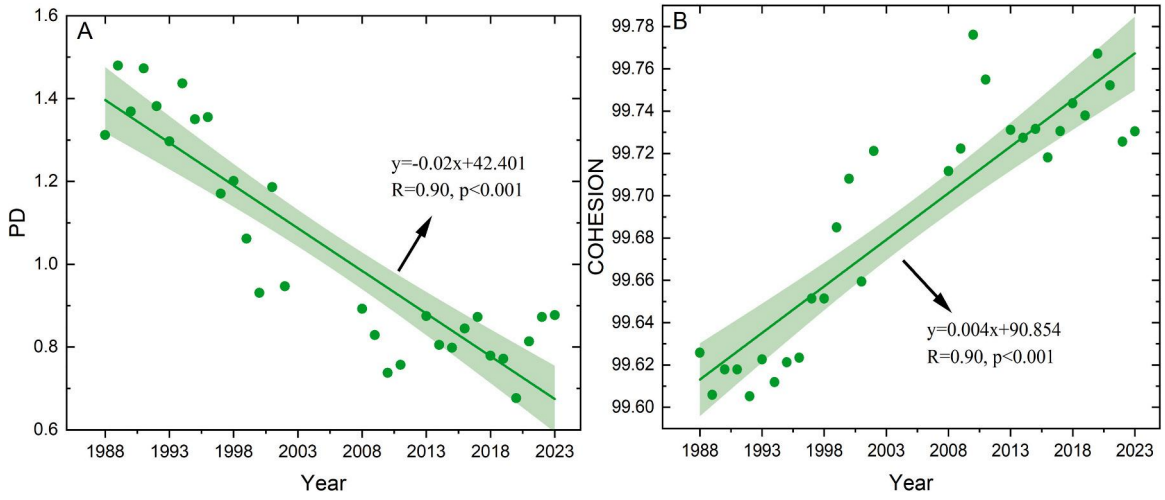

Fig. 8. Changes in landscape indices of mangrove forest in the Indus Delta. (A) Patch Density (PD). (B) COHESION index.

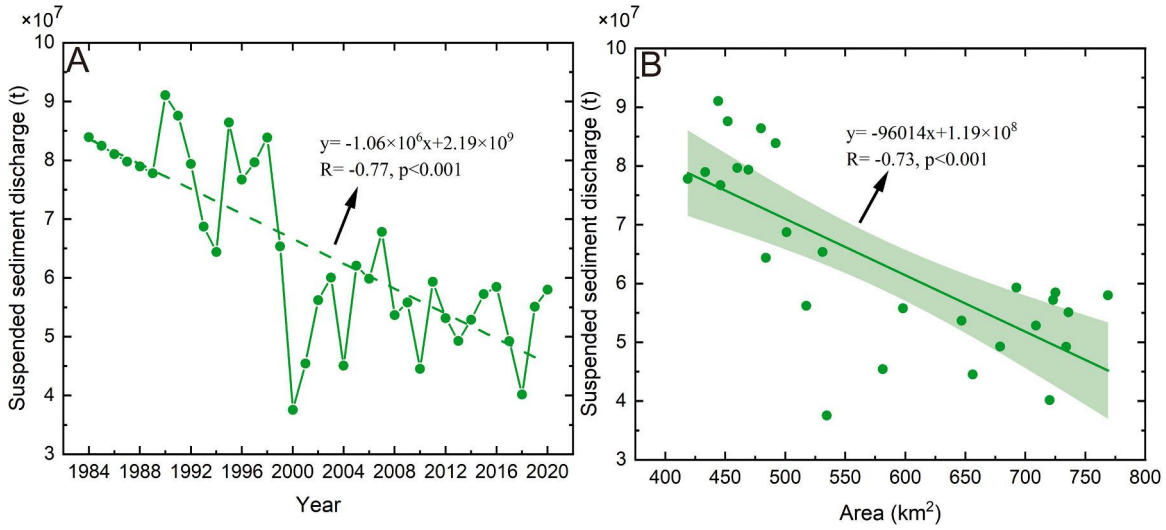

Fig. 9. (A) Changes in upstream suspended sediment transport from 1984 to 2020. (B) Relationship between the area of mangrove forests and suspended sediment discharge.

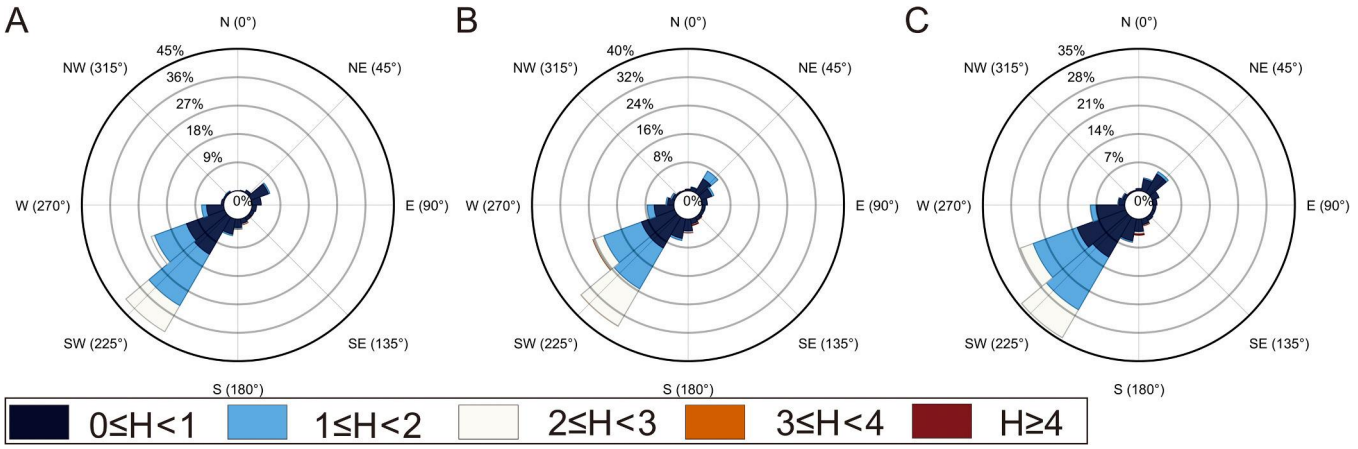

Fig. 10. Wave characteristics in different regions of the Indus Delta. (A) Northwest Part. (B) Southwest Part. (C) South Part.

survival in high-salinity environments (Liang et al., 2008). Additionally, the aerenchyma in the pneumatophores of mangrove plants ensures their survival during tidal submersion (Srikanth et al., 2016), resulting in the aggregation of mangrove patches along the tidal channels in the northwest (Fig. 5H), as evidenced by the linear growth in the aggregation index from 1988 to 2023 (Fig. 8B). The changes in the tidal channels in the southwest and south differ from those in the northwest. Cross-sectional analysis from 1988 to 2023 revealed that the width of the southwest cross-section (Transect B) decreased from 344 m in 1988 to 0 m in 2023, while the southern cross-section (Transect C) decreased from 176 m to 29 m. Over this period, the tidal channels in the southwest and south gradually narrowed, with some channels completely closing (Figs. 13B, 13C). This continuous closure of the tidal channels facilitated the extension of mangrove roots and the growth of mangrove seedlings, further stabilizing these ecosystems.

Sea level rise, accelerating coastal submergence and prompting landward mangrove migration, further influences mangrove dynamics (Gilman et al., 2008; Ellison, 2012). Among Pakistan's existing tide gauge stations, the Karachi tide gauge station possesses the longest time series of observational data, recording both tidal and sea level data (Weeks et al., 2023). According to sea level data from the Permanent Service for Mean Sea Level, the trend of sea level rise in Pakistan is 2.01 mm/yr, indicating that Pakistan is facing the threat of rising sea levels. In the southwest and south parts of the Indus Delta, seaward erosion may be attributed to this rising sea level.

4.3. *Impacts of anthropogenic activities*

The Red River Delta and the Irrawaddy Delta in Southeast Asia are primarily influenced by monsoon climates. In contrast, the Indus Delta is affected by a subtropical desert climate and hosts the world's largest arid mangrove ecosystems, predominantly composed of Avicennia marina (Irfan Aziz and Khan, 2000). Resource scarcity in these deltas has driven the migration of approximately 90,000 individuals, and seawater intrusion has resulted in the disappearance of about 120 villages (Memon, 2005). The limited availability of habitable land implies that human activities have a relatively minor direct impact on the arid mangroves of the Indus Delta (Adame et al., 2021).

A significant anthropogenic threat to mangroves in the Indus Delta is the large-scale discharge of oil. Mangroves, as part of tidal wetlands, are particularly susceptible to extensive and prolonged oil spills (Duke, 2016). Mangroves affected by oil spills are deprived of essential oxygen, leading to widespread mortality (Kairo et al., 2005). The Korangi Creek area of the delta and the nearby Karachi Port have suffered from severe marine oil pollution, with approximately 20,000 tons of oil contaminating Pakistan's coastal areas annually. The sources of this pollution include ship leaks and bilge cleaning operations (Saifullah, 1997). While oil pollution affects various areas of the delta, Korangi Creek, situated at

Fig. 11. Steep escarpments formed by wave action in the Indus Delta. (A) Source: WWF-Pakistan 2012. (B) Source: Google Earth.

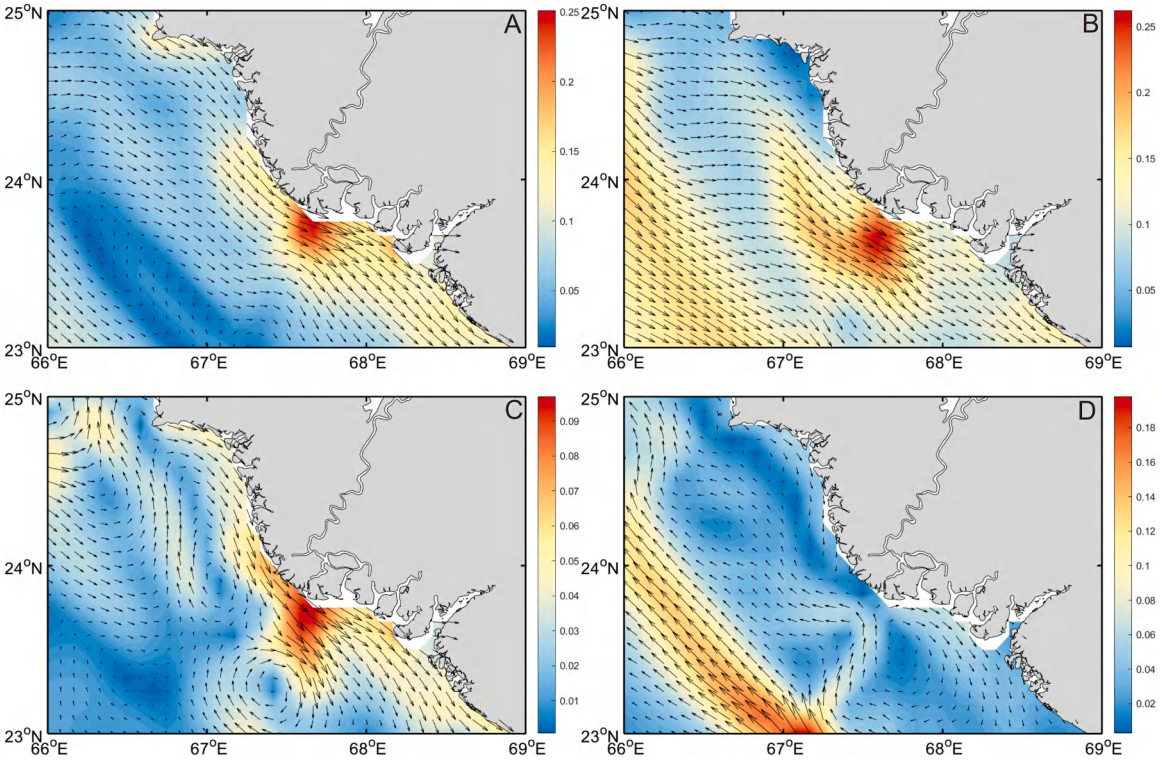

Fig. 12. Seasonal variation in tidal current along the Indus Delta. (A) Spring. (B) Summer. (C) Autumn. (D) Winter.

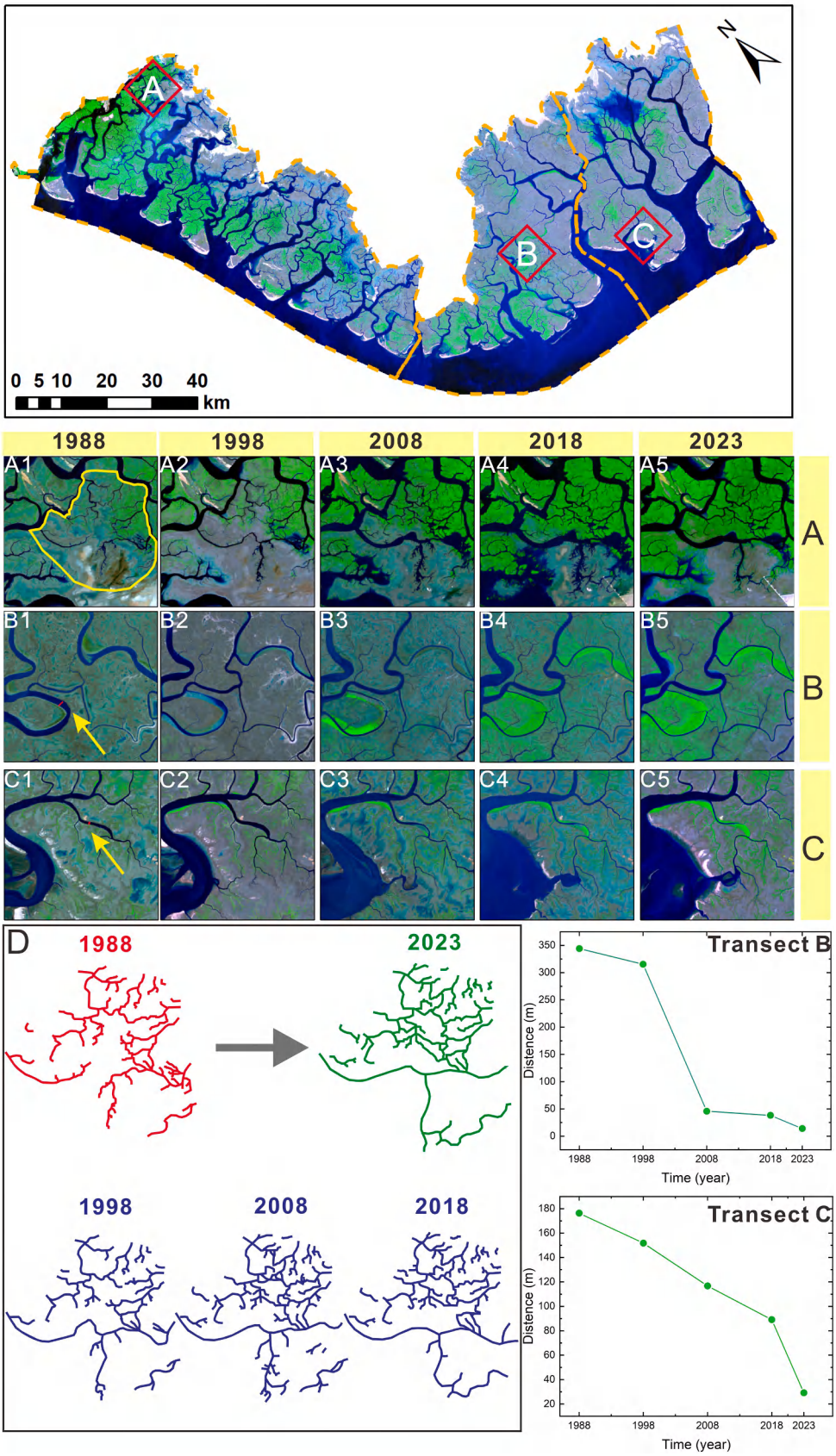

Fig. 13. Patterns of landward expansion of mangroves in the three regions from 1988 to 2023. (A) Northwest Part. (B) Southwest Part. (C) South Part. (D) Extension connections of tidal channels in the Northwest Part with transects B and C.

the delta's northernmost point (Fig. 1B), exhibits significant mangrove loss at its northwestern tip (Fig. 5H), making it the most significantly affected area by oil spill-induced mangrove degradation.

In response to these challenges, Pakistan began mangrove plantation activities in coastal areas in 2006, coupled with enhanced community outreach and eco-tourism efforts to protect mangroves in the delta (Saeed et al., 2019). The extensive mudflats of the Indus Delta provide suitable sites for mangrove restoration, with notable mangrove plantations established in the northwest and southwest areas of Keti Bunder and Shah Bunder (Masood et al., 2015). Both areas have shown positive outcomes since the onset of these mangrove planting activities in 2006. The planned mangrove forests have become increasingly concentrated and have gradually spread (Fig. 14). Photographic evidence from fixed points in Keti Bunder taken in May 2010 and May 2012 further supports this trend (Fig. 15). This reforestation effort likely accounts for the relative increase in mangrove area in the northwest and southwest since 2008.

4.4. Comparison with other regions

In the Indo-Pacific region, the imbalance between the rate of sea-level rise and surface elevation growth poses a significant threat to the sustainable growth of mangroves. In areas without anthropogenic barriers, mangroves can migrate inland to mitigate submersion rates (Lovelock et al., 2015). Similar landward retreats of mangrove shorelines have been observed in the Mekong Delta of Southeast Asia and the Ganges Delta of South Asia (Besset et al., 2019; Samanta et al., 2021). The Indus Delta mirrors this phenomenon, particularly in its southwest and southern regions, where sea-level rise contributes to mangrove erosion. However, in the Indus Delta, the erosion caused by the strong southwest waves may exceed the impact of sea-level rise.

Conversely, some studies report a trend of seaward expansion of mangroves. For instance, Long et al. (2022) observed seaward expansion of mangroves in the Nanliu River Delta, the largest delta in the Beibu Gulf of China. This tide-dominated delta benefits from significant sediment deposition by tidal flows, which extends the mangrove growth range. Similarly, the Irrawaddy River Delta in Southeast Asia exhibits seaward expansion of mangroves, where barrier islands at the estuary effectively protect the mangroves from the impact of strong waves (Xiong et al., 2024). In contrast, the Indus Delta is influenced by both waves and tidal currents. Coastal erosion dominates when wave action is predominant, leading to mangrove shoreline retreat. However, when tidal and wave actions are relatively strong, a synergistic "wave stirring and tidal transport" effect occurs, where waves and tides together transport sediment landward, thereby creating suitable habitats for mangrove growth (Long et al., 2022). This dual influence is evident in the Indus Delta, where sediment transport driven by the interaction of waves and tides supports mangrove expansion in specific areas.

4.5. Uncertainty analysis

This study explores the long-term trends and spatiotemporal changes in the mangroves of the Indus Delta using machine learning techniques and remote sensing images. Despite the robustness of the methodology, several uncertainties need to be addressed, including potential errors in data sources and during the processing stages. One significant source of uncertainty is the 30 m spatial resolution of Landsat data, which introduces a pixel error of approximately 9×10^{-4} km^2. However, given the large scale of the study area, this error is effectively mitigated (Okin and Gu, 2015). The minimum recorded area of the Indus Delta mangroves (433.22 km^2) is far greater than the pixel error, indicating that the pixel error has a negligible impact on the overall accuracy of mangrove area calculations. A limitation of this study is the absence of available remote sensing images for the periods 2003–2007 and 2012. These temporal gaps introduce discontinuities in the analysis of mangrove change trends, thereby affecting the continuity of long-term trend assessments. The wave data from the European Centre for Medium-Range Weather Forecasts (ECMWF) and the current data from the Copernicus Marine Environment Monitoring Service (CMEMS) used in this study have high spatial and temporal resolutions (e.g., hourly data). While these datasets generally provide reliable insights, they may exhibit systematic biases during anomalous climate events or extreme environmental conditions, which could influence the study's conclusions regarding hydrodynamic influences on mangrove dynamics. Moreover, the Random Forest algorithm is an ensemble model composed of multiple decision trees, each of which may carry some biases, and these biases can accumulate in the final classification results. Therefore, we employed the Error Matrix Method (Foody, 2002) and combined it with the validation dataset to assess the performance of the classification model. The overall accuracy and Kappa coefficient generated by this method can be used to demonstrate the relationship between the model's predictions on the test dataset and the actual values. The evaluation of mangrove recognition accuracy mainly relies on the overall accuracy and Kappa coefficient, both of which range between 0 and 1. Accuracy values greater than 0.8 are considered reliable, while those below 0.4 indicate low accuracy (Foody, 2010). In this study, the annual overall accuracies and Kappa coefficients consistently exceed 0.90 and 0.80, respectively (Table 1), demonstrating high reliability and accuracy in the identification results. In summary, while this study provides a robust analysis of mangrove dynamics in the Indus Delta, the identified uncertainties—stemming from data resolution, temporal gaps, potential biases in wave and current data, and model classification—should be acknowledged. These factors highlight the need for cautious interpretation of the results and underscore the importance of continuous methodological refinement.

5. Conclusions

As one of the largest deltas in the world and home to the most extensive arid climate mangrove system, the Indus Delta mangroves hold significant ecological importance. This research provides a comprehensive temporal and spatial analysis of mangrove dynamics in the Indus Delta from 1988 to 2023. The key findings are as follows:

1. From 1988–2023, the overall area of mangroves in the Indus Delta exhibited a positive trend, with an average annual increase of 11.58 km^2. The mangrove area in the three regions of the delta showed different changing trends: in the northwest part, rapid growth was observed before 2002, followed by a deceleration of growth from 2008 to 2023. The southwest part displayed an initial slow growth phase, succeeded by rapid growth in the latter period. The southern part did not show a distinct trend.
2. The spatial distribution of mangroves in the delta tends to be concentrated. Mangrove expansion predominantly occurred in the landward areas, extending along tidal channels, while losses were concentrated in the seaward areas. The mangrove shoreline retreated landward at a rate of 4.7 m per year. Among the three regions, the southwest part experienced the most severe erosion, the south part maintained a balance between erosion and expansion, and the northwest part experienced the least erosion.
3. The Indus Delta is subject to the combined influences of waves and tidal currents, with the primary mechanism for nearshore sediment transport being "wave stirring and tidal transport". Rising sea levels and southwest waves significantly contribute to the erosion observed in the southwest part of the study area. The southwest and south parts of the delta are heavily affected by tidal currents throughout the year, facilitating mangrove growth along tidal channels. In the northwest part, the river channels extend and connect, transforming mudflats into mangroves, whereas tidal channels in the southwest and south parts show gradual closure, providing additional growing space for mangroves.

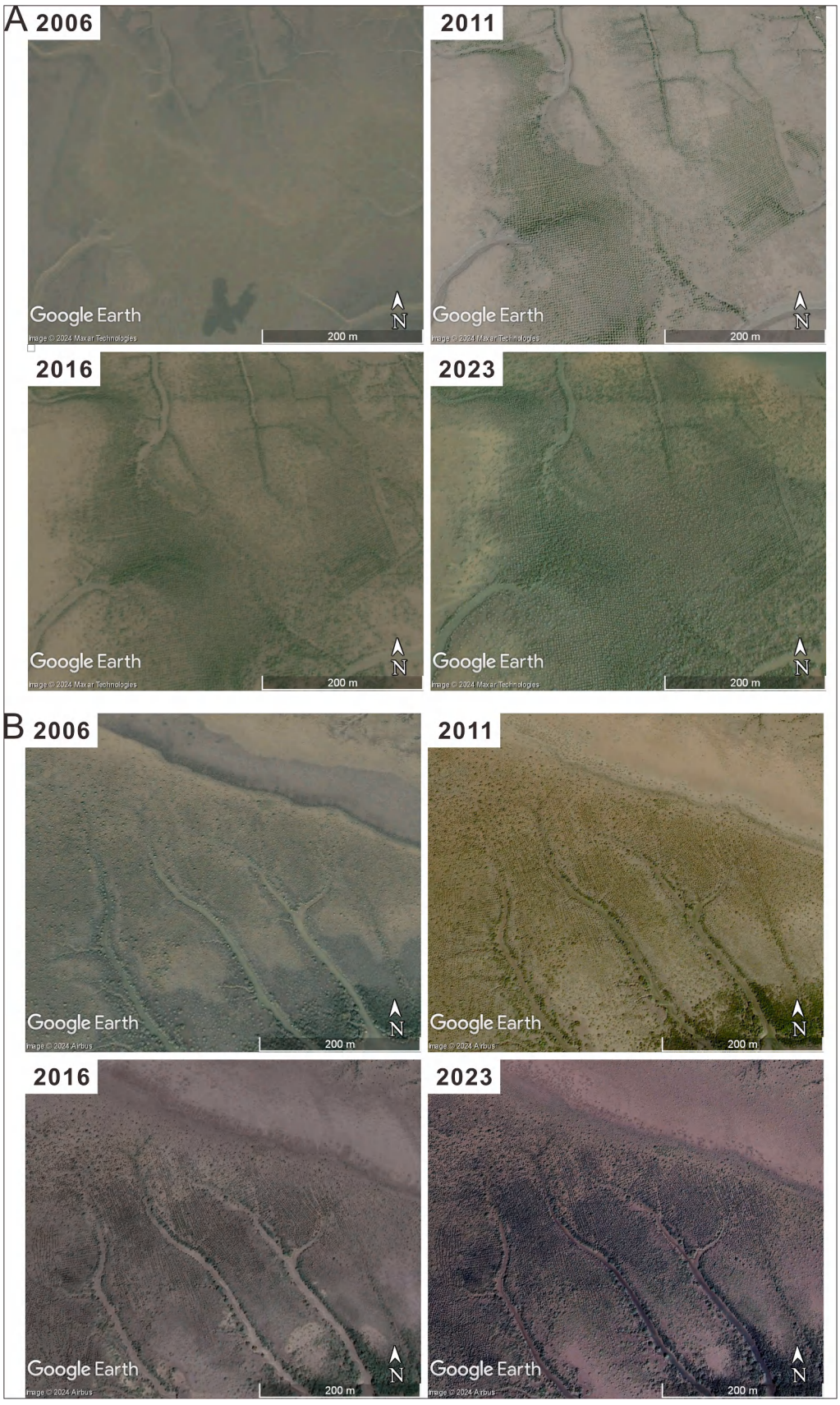

Fig. 14. Changes in mangrove plantations at Keti Bunder (A) and Shah Bunder (B) from 2006 to 2023. Source: Google Earth.

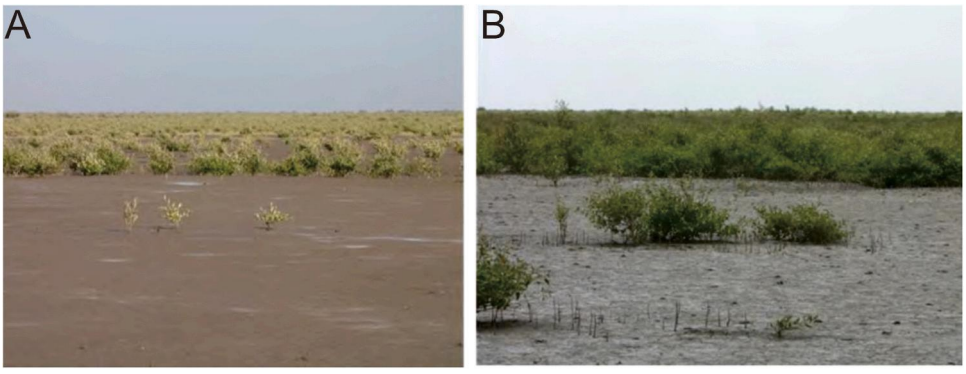

Fig. 15. Photographs of the mangrove site in Keti Bunder taken in May 2010 (A) and May 2012 (B). Source: WWF-Pakistan 2012.

Table 1
Accuracy assessment of research area.

Year	Overall accuracy	Kappa coefficient value
1988	0.91	0.87
1989	0.97	0.96
1990	0.96	0.92
1991	0.98	0.97
1992	0.98	0.96
1993	0.98	0.96
1994	0.95	0.90
1995	0.95	0.90
1996	0.91	0.83
1997	0.97	0.95
1998	0.98	0.97
1999	0.92	0.86
2000	0.97	0.95
2001	0.99	0.98
2002	0.97	0.95
2008	0.90	0.85
2009	0.96	0.94
2010	0.90	0.82
2011	0.99	0.98
2013	0.96	0.92
2014	0.96	0.93
2015	0.98	0.97
2016	0.98	0.96
2017	0.98	0.97
2018	0.96	0.93
2019	0.97	0.95
2020	0.98	0.97
2021	0.98	0.97
2022	0.97	0.95
2023	0.97	0.93

Moreover, the Indus Delta, under the influence of a subtropical desert climate, exhibits unique characteristics compared to deltas affected by monsoon climates. It supports the world's largest mangroves in an arid climate. The low human habitation and land use in the delta result in minimal direct human interference with the mangroves. Anthropogenic impacts are primarily localized, with oil spills from ports causing mangrove mortality and mangrove restoration efforts through plantations contributing to their recovery. In conclusion, this study underscores the dynamic nature of the Indus Delta mangroves and highlights the critical role of both natural and anthropogenic factors in shaping their temporal and spatial patterns.

CRediT authorship contribution statement

Jinping Cheng: Writing – review & editing, Methodology, Formal analysis. **Xixing Liang:** Resources, Methodology, Data curation. **Ying Zhou:** Writing – original draft, Software, Resources, Methodology, Investigation, Data curation. **Zhijun Dai:** Writing – review & editing, Writing – original draft, Supervision, Software, Resources, Methodology, Investigation, Funding acquisition, Conceptualization.

Declaration of Competing Interest

The authors declare that there is no conflicts of interest regarding the submitted paper of "Machine learning-based monitoring of mangrove ecosystem dynamics in the Indus Delta".

Data Availability

Data will be made available on request.

Acknowledgments

This research was supported by the National Natural Science Key Foundation of China (NSFC) (41930537), National Key R&D Program of China (2023YFE0121200), Shanghai International Science and Technology Cooperation Fund Project (23230713800), International Joint Laboratory of Estuarine and Coastal Research, Shanghai (21230750600), and Research Scheme of the University Research Facility of Data Science & Artificial Intelligence at the Education University of Hong Kong (CB384).

References

Adame, M., Reef, R., Santini, N., Najera, E., Turschwell, M., Hayes, M., Masque, P., Lovelock, C., 2021. Mangroves in arid regions: ecology, threats, and opportunities. Estuar., Coast. Shelf Sci. 248, 106796.
Ahmad, S., Center, S.A., 2012. Water insecurity: a threat for Pakistan and India. JSTOR.
Amjad, A.S., Jusoff, K., 2007. Mangrove conservation through community participation in Pakistan: the case of Sonmiani Bay. Int J. Syst. Appl. Eng. Dev. 1, 75–81.
Anthony, E., Goichot, M., 2020. Sediment flow in the context of mangrove restoration and conservation. A BMZ, IUCN and WWF project. A rapid assessment guidance manual.
Belgiu, M., Drăguţ, L., 2016. Random forest in remote sensing: A review of applications and future directions. ISPRS J. Photogramm. Remote Sens. 114, 24–31.
Besset, M., Gratiot, N., Anthony, E.J., Bouchette, F., Goichot, M., Marchesiello, P., 2019. Mangroves and shoreline erosion in the Mekong River delta, Viet Nam. Estuar., Coast. Shelf Sci. 226, 106263.
Blankespoor, B., Dasgupta, S., Lange, G.-M., 2017. Mangroves as a protection from storm surges in a changing climate. Ambio 46, 478–491.
Bryan-Brown, D.N., Connolly, R.M., Richards, D.R., Adame, F., Friess, D.A., Brown, C.J., 2020. Global trends in mangrove forest fragmentation. Sci. Rep. 10, 7117.
Bunting, P., Hilarides, L., Rosenqvist, A., Lucas, R.M., Kuto, E., Gueye, Y., Ndiaye, L., 2023. Global mangrove watch: monthly alerts of mangrove loss for Africa. Remote Sens. 15, 2050.
Chaudhuri, P., Chaudhuri, S., Ghosh, R., 2019. The role of mangroves in coastal and estuarine sedimentary accretion in Southeast Asia. Sedimentary Processes-Examples from Asia, Turkey and Nigeria, 203-218.
Contessa, V., Dyson, K., Vivar Mulas, P.P., Kindgard, A., Liu, T., Saah, D., Tenneson, K., Pekkarinen, A., 2023. Uncovering dynamics of global mangrove gains and losses. Remote Sens. 15, 3872.
Day, J., Goodman, R., Chen, Z., Hunter, R., Giosan, L., Wang, Y., 2021. Deltas in arid environments. Water 13, 1677.
Dethier, E.N., Renshaw, C.E., Magilligan, F.J., 2022. Rapid changes to global river suspended sediment flux by humans. Science 376, 1447–1452.

Duke, N.C., 2016. Oil spill impacts on mangroves: recommendations for operational planning and action based on a global review. Mar. Pollut. Bull. 109, 700–715.
Ellison, A.M., Felson, A.J., Friess, D.A., 2020. Mangrove rehabilitation and restoration as experimental adaptive management. Front. Mar. Sci. 7, 327.
Ellison, J., 2012. Climate change vulnerability assessment and adaptation planning for mangrove systems. In. University Of Tasmania.
Ellison, J.C., 2021. Factors influencing mangrove ecosystems. Mangrove.: Ecol., Biodivers. Manag. 97–115.
Ezcurra, P., Ezcurra, E., Garcillán, P.P., Costa, M.T., Aburto-Oropeza, O., 2016. Coastal landforms and accumulation of mangrove peat increase carbon sequestration and storage. Proc. Natl. Acad. Sci. 113, 4404–4409.
FAO, 2007. Food and Agriculture Organization of the United Nations In The world's mangroves 1980–2005. Forest Resources Division, FAO. FAO Forestry Paper, Rome, p. 153.
FAO. 2020. Global Forest Resources Assessment 2020: Main report. Rome.
Fernández-Delgado, M., Cernadas, E., Barro, S., Amorim, D., 2014. Do we need hundreds of classifiers to solve real world classification problems? J. Mach. Learn. Res. 15, 3133–3181.
Field, C.D., 1995. Impact of expected climate change on mangroves. In, Asia-Pacific Symposium on Mangrove Ecosystems: Proceedings of the International Conference held at The Hong Kong University of Science & Technology, September 1–3, 1993. Springer, pp. 75-81.
Foody, G.M., 2002. Status of land cover classification accuracy assessment. Remote Sens. Environ. 80, 185–201.
Foody, G.M., 2010. Assessing the accuracy of land cover change with imperfect ground reference data. Remote Sens. Environ. 114, 2271–2285.
Gerona-Daga, M.E.B., Salmo III, S.G., 2022. A systematic review of mangrove restoration studies in Southeast Asia: Challenges and opportunities for the United Nation's Decade on Ecosystem Restoration. Front. Mar. Sci. 9, 987737.
Gilman, E., Ellison, J., Coleman, R., 2007. Assessment of mangrove response to projected relative sea-level rise and recent historical reconstruction of shoreline position. Environ. Monit. Assess. 124, 105–130.
Gilman, E.L., Ellison, J., Duke, N.C., Field, C., 2008. Threats to mangroves from climate change and adaptation options: a review. Aquat. Bot. 89, 237–250.
Giosan, L., Constantinescu, S., Clift, P.D., Tabrez, A.R., Danish, M., Inam, A., 2006. Recent morphodynamics of the Indus delta shore and shelf. Cont. Shelf Res. 26, 1668–1684.
Giri, C., Ochieng, E., Tieszen, L.L., Zhu, Z., Singh, A., Loveland, T., Masek, J., Duke, N., 2011. Status and distribution of mangrove forests of the world using earth observation satellite data. Glob. Ecol. Biogeogr. 20, 154–159.
Goldberg, L., Lagomasino, D., Thomas, N., Fatoyinbo, T., 2020. Global declines in human-driven mangrove loss. Glob. Change Biol. 26, 5844–5855.
Habibullah, I., Sanjaya, H., Putra, I.N.G., 2023. Utilization of the Indices to Detect and Monitor the Landcover Changes of Mangroves. In, IOP Conference Series: Earth and Environmental Science. IOP Publishing, p. 012033.
Hadi, A., 2019. Dams and Destruction: The Case Study of Indus Delta, Sindh, Pakistan. Environ. Justice 12, 48–60.
Hagger, V., Worthington, T.A., Lovelock, C.E., Adame, M.F., Amano, T., Brown, B.M., Friess, D.A., Landis, E., Mumby, P.J., Morrison, T.H., 2022. Drivers of global mangrove loss and gain in social-ecological systems. Nat. Commun. 13, 6373.
Inam, A., Clift, P.D., Giosan, L., Tabrez, A.R., Tahir, M., Rabbani, M.M., Danish, M., 2007. The geographic, geological and oceanographic setting of the Indus River. Large River.: Geomorphol. Manag. 1 333–346.
Irfan Aziz, I.A., Khan, M., 2000. Physiological adaptations of Avicennia marina to seawater concentrations in the Indus delta, Pakistan.
Jia, M., Wang, Z., Mao, D., Ren, C., Song, K., Zhao, C., Wang, C., Xiao, X., Wang, Y., 2023. Mapping global distribution of mangrove forests at 10-m resolution. Sci. Bull. 68, 1306–1316.
Kairo, J., Bosire, J., Omar, M., 2005. Assessment of the Effects of Oil Spill on the Mangrove Forests of Port Reitz, Mombasa.
Kalhoro, N., He, Z., Xu, D., Faiz, M., Yafei, L., Sohoo, N., Bhutto, A., 2016. Vulnerability of the Indus River Delta of the north Arabian Sea, Pakistan. Glob. NEST J. 18, 599–610.
Karrar, H., 2021. The Indus delta between past and future: precarious livelihoods and neoliberal imaginaries in a Parched Coastal Belt. J. Indian Ocean World Stud. 5, 47–67.
Lee, K.-Y., Shih, S.S., Huang, Z.-Z., 2022. Mangrove colonization on tidal flats causes straightened tidal channels and consequent changes in the hydrodynamic gradient and siltation potential. J. Environ. Manag. 314, 115058.
Liang, S., Zhou, R., Dong, S., Shi, S., 2008. Adaptation to salinity in mangroves: Implication on the evolution of salt-tolerance. Chinese. Sci. Bull. 53, 1708–1715.
Liu, X., Fatoyinbo, T.E., Thomas, N.M., Guan, W.W., Zhan, Y., Mondal, P., Lagomasino, D., Simard, M., Trettin, C.C., Deo, R., 2021. Large-scale high-resolution coastal mangrove forests mapping across West Africa with machine learning ensemble and satellite big data. Front. Earth Sci. 8, 560933.
Long, C., Dai, Z., Zhou, X., Mei, X., Mai Van, C., 2021. Mapping mangrove forests in the Red River Delta, Vietnam. For. Ecol. Manag. 483.
Long, C., Dai, Z., Wang, R., Lou, Y., Zhou, X., Li, S., Nie, Y., 2022. Dynamic changes in mangroves of the largest delta in northern Beibu Gulf, China: reasons and causes. For. Ecol. Manag. 504.
Lovelock, C.E., Cahoon, D.R., Friess, D.A., Guntenspergen, G.R., Krauss, K.W., Reef, R., Rogers, K., Saunders, M.L., Sidik, F., Swales, A., 2015. The vulnerability of Indo-Pacific mangrove forests to sea-level rise. Nature 526, 559–563.
Maiti, S.K., Chowdhury, A., 2013. Effects of anthropogenic pollution on mangrove biodiversity: a review. J. Environ. Prot. 2013.
Masood, H., Afsar, S., Zamir, U.B., Kazmi, J.H., 2015. Application of comparative remote sensing techniques for monitoring mangroves in Indus Delta, Sindh, Pakistan. In, Biological Forum. Research Trend, p. 783.
McGarigal, K., Cushman, S.A., Neel, M.C., Ene, E., 2002. Spatial pattern analysis program for categorical maps. URL: www. umass. edu/landeco/research/fragstats/fragstats. html.
Memon, A.A., 2005. Devastation of the Indus river delta. In, Impacts of global climate change, pp. 1-12.
Mukhtar, I., Hannan, A., 2012. Constrains on mangrove forests and conservation projects in Pakistan. J. Coast. Conserv. 16, 51–62.
Nrothwest, P., 1995. FRAGSTATS: spatial pattern analysis program for quantifying landscape structure. In.
Okin, G.S., Gu, J., 2015. The impact of atmospheric conditions and instrument noise on atmospheric correction and spectral mixture analysis of multispectral imagery. Remote Sens. Environ. 164, 130–141.
Paling, E., Kobryn, H., Humphreys, G., 2008. Assessing the extent of mangrove change caused by Cyclone Vance in the eastern Exmouth Gulf, northwestern Australia. Estuar., Coast. Shelf Sci. 77, 603–613.
Pham, T.D., Yokoya, N., Bui, D.T., Yoshino, K., Friess, D.A., 2019. Remote sensing approaches for monitoring mangrove species, structure, and biomass: Opportunities and challenges. Remote Sensing 11, 230.
Poortinga, A., Aekakkararungroj, A., Kityuttachai, K., Nguyen, Q., Bhandari, B., Soe Thwal, N., Priestley, H., Kim, J., Tenneson, K., Chishtie, F., 2020. Predictive analytics for identifying land cover change hotspots in the mekong region. Remote Sensing 12, 1472.
Rahman, M.K., Crawford, T.W., Islam, M.S., 2022. Shoreline change analysis along rivers and deltas: A systematic review and bibliometric analysis of the shoreline study literature from 2000 to 2021. Geosciences 12, 410.
Raju, R.D., Arockiasamy, M., 2022. Coastal protection using integration of mangroves with floating barges: An innovative concept. J. Mar. Sci. Eng. 10, 612.
Reynaud, J.-Y., Dalrymple, R.W., 2012. Shallow-marine tidal deposits. Princ. Tidal Sedimentol. 335–369.
Richards, D.R., Friess, D.A., 2016. Rates and drivers of mangrove deforestation in Southeast Asia, 2000–2012. National Academy of Sciences.
Saeed, U., Ahmad, S.R., Gilani, H., Nawaz, R., Shahzad, N., Ashraf, I., Qazi, W.A., 2019. Monitoring mangroves plantation sites through integration of repeat terrestrial photographs and spaceborne imagery.
Saifullah, S., 1997. Management of the Indus Delta mangroves. In, Coastal zone management imperative for maritime developing nations. Springer, pp. 333-346.
Samanta, S., Hazra, S., Mondal, P.P., Chanda, A., Giri, S., French, J.R., Nicholls, R.J., 2021. Assessment and attribution of mangrove Forest changes in the Indian Sundarbans from 2000 to 2020. Remote Sens. 13, 4957.
Shapiro, A.C., Trettin, C.C., Küchly, H., Alavinapanah, S., Bandeira, S., 2015. The mangroves of the Zambezi Delta: Increase in extent observed via satellite from 1994 to 2013. Remote Sens. 7, 16504–16518.
Sheykhmousa, M., Mahdianpari, M., Ghanbari, H., Mohammadimanesh, F., Ghamisi, P., Homayouni, S., 2020. Support vector machine versus random forest for remote sensing image classification: A meta-analysis and systematic review. IEEE J. Sel. Top. Appl. Earth Obs. Remote Sens. 13, 6308–6325.
Šímová, P., Gdulová, K., 2012. Landscape indices behavior: A review of scale effects. Appl. Geogr. 34, 385–394.
Siyal, A.A., Solangi, G.S., Siyal, P., Babar, M.M., Ansari, K., 2022. Shoreline change assessment of Indus delta using GIS-DSAS and satellite data. Reg. Stud. Mar. Sci. 53, 102405.
Slamet, N.S., Dargusch, P., Aziz, A.A., Wadley, D., 2020. Mangrove vulnerability and potential carbon stock loss from land reclamation in Jakarta Bay, Indonesia. Ocean Coast. Manag. 195, 105283.
Song, S., Ding, Y., Li, W., Meng, Y., Zhou, J., Gou, R., Zhang, C., Ye, S., Saintilan, N., Krauss, K.W., 2023. Mangrove reforestation provides greater blue carbon benefit than afforestation for mitigating global climate change. Nat. Commun. 14, 756.
Spalding, M., Mcivor, A., Tonneijck, F., Tol, S., Eijk, Pv, 2014. Mangroves for coastal defence.
Srikanth, S., Lum, S.K.Y., Chen, Z., 2016. Mangrove root: adaptations and ecological importance. Trees 30, 451–465.
Syed, N., Siddiqa, T., 2019. The study of tidal current dynamics and impact of bathymetry in training the currents along the coast of Karachi, Pakistan. Int. J. Mar. Sci. Ocean Technol. https://doi. org/10.19070/2577-4395-1900015.
Tang, Z., Li, Y., Gu, Y., Jiang, W., Xue, Y., Hu, Q., LaGrange, T., Bishop, A., Drahota, J., Li, R., 2016. Assessing Nebraska playa wetland inundation status during 1985–2015 using Landsat data and Google Earth Engine. Environ. Monit. Assess. 188.
Teluguntla, P., Thenkabail, P.S., Oliphant, A., Xiong, J., Gumma, M.K., Congalton, R.G., Yadav, K., Huete, A., 2018. A 30-m landsat-derived cropland extent product of Australia and China using random forest machine learning algorithm on Google Earth Engine cloud computing platform. ISPRS J. Photogramm. Remote Sens. 144, 325–340.
Thieler, E.R., Himmelstoss, E.A., Zichichi, J.L., Ergul, A., 2009. The Digital Shoreline Analysis System (DSAS) version 4.0-an ArcGIS extension for calculating shoreline change. In. US Geological Survey.
Visschers, L.L., Santos, C.D., Franco, A.M., 2022. Accelerated migration of mangroves indicate large-scale saltwater intrusion in Amazon coastal wetlands. Sci. Total Environ. 836, 155679.
Wang, H., Peng, Y., Wang, C., Wen, Q., Xu, J., Hu, Z., Jia, X., Zhao, X., Lian, W., Temmerman, S., 2021. Mangrove loss and gain in a densely populated urban estuary: lessons from the Guangdong-Hong Kong-Macao Greater Bay Area. Front. Mar. Sci. 8, 693450.

Wang, L., Jia, M., Yin, D., Tian, J., 2019. A review of remote sensing for mangrove forests: 1956–2018. Remote Sens. Environ. 231, 111223.
Ward, R.D., Friess, D.A., Day, R.H., Mackenzie, R.A., 2016. Impacts of climate change on mangrove ecosystems: a region by region overview. Ecosyst. Health Sustain. 2, e01211.
Weeks, J.H., Ahmed, S.N., Daron, J.D., Harrison, B.J., Hogarth, P., Ibrahim, T., Inam, A., Khan, A., Khan, F.A., Khan, T.M.A., 2023. Sea-level rise in Pakistan: recommendations for strengthening evidence-based coastal decision-making. Hydrology 10, 205.
Woodroffe, C., 1992. Mangrove sediments and geomorphology. Trop. Mangrove Ecosyst. 41, 7–41.
Worthington, T.A., Andradi-Brown, D.A., Bhargava, R., Buelow, C., Bunting, P., Duncan, C., Fatoyinbo, L., Friess, D.A., Goldberg, L., Hilarides, L., 2020. Harnessing big data to support the conservation and rehabilitation of mangrove forests globally. One Earth 2, 429–443.
Wulder, M.A., Loveland, T.R., Roy, D.P., Crawford, C.J., Masek, J.G., Woodcock, C.E., Allen, R.G., Anderson, M.C., Belward, A.S., Cohen, W.B., 2019. Current status of Landsat program, science, and applications. Remote Sens. Environ. 225, 127–147.
Xiong, Y., Dai, Z., Long, C., Liang, X., Lou, Y., Mei, X., Nguyen, B.A., Cheng, J., 2024. Machine Learning-Based examination of recent mangrove forest changes in the western Irrawaddy River Delta, Southeast Asia. Catena 234, 107601.
Yang, G., Huang, K., Sun, W., Meng, X., Mao, D., Ge, Y., 2022a. Enhanced mangrove vegetation index based on hyperspectral images for mapping mangrove. ISPRS J. Photogramm. Remote Sens. 189, 236–254.
Yang, L., Driscol, J., Sarigai, S., Wu, Q., Chen, H., Lippitt, C.D., 2022b. Google Earth Engine and Artificial Intelligence (AI): A Comprehensive Review. Remote Sens. 14.
You, H., Liu, Y., Lei, P., Qin, Z., You, Q., 2023. Segmentation of individual mangrove trees using UAV-based LiDAR data. Ecol. Inform. 77, 102200.
Zablan, C.D.C., Blanco, A.C., Nadaoka, K., 2023. Temporal Variation of Threshold Segmentation-Based Mangrove Mapping Indices in Karimunjawa-Kemujan Islands with Sentinel Images. In, IGARSS 2023-2023 IEEE International Geoscience and Remote Sensing Symposium. IEEE, pp. 5316-5319.
Zhang, Y., Hou, X., 2020. Characteristics of coastline changes on southeast Asia Islands from 2000 to 2015. Remote Sens. 12, 519.
Zheng, J., Sun, C., Zhao, S., Hu, M., Zhang, S., Li, J., 2023. Classification of salt marsh vegetation in the Yangtze River Delta of China using the pixel-level time-series and XGBoost algorithm. J. Remote Sens. 3, 0036.